

# Year Eight Project Report



<b>Project ID: R1-B2</b>					
<b>Title: Wave-Based Computational Modeling for Detection of Tumors, Buried Objects and Subcellular Structures</b>					
<b>Investigator Name</b>	<b>Dept</b>	<b>Institution</b>	<b>Email</b>	<b>Phone</b>	<b>Fax</b>
Carey Rappaport (PL)	ECE	NEU	rappaport@neu.edu	617.373.2043	617.373.8627
Ann Morgenthaler	ECE	NEU	rappapor@yahoo.com	781.237.6864	617.373.8627
Purnima Ratilal	ECE	NEU	purnima@ece.neu.edu	617.373.5110	617.373.8627
Sophia Zhan	ECE	NEU	hzhan@coe.neu.edu	617.373.4874	617.373.8627
Jose Angel Martinez	ECE	NEU	jmartine@ece.neu.edu	617.373.2847	617.373.8627
<b>Graduate Student Name</b>	<b>Major</b>	<b>Institution</b>	<b>Email</b>	<b>Masters or PhD Candidate</b>	<b>Anticipated Graduation Date</b>
Ersel Karbayez	ECE	NEU	ekarbeya@ece.neu.edu	PhD	2008
Qiuzhao Dong	ECE	NEU	qzdong@ece.neu.edu	PhD	2008
Maryam Jalalinia	ECE	NEU	m_jalalinia@yahoo.com	MS	2007
Richie Sullivan	ECE	NEU	rsulliva@ece.neu.edu	MS	2007
Johanna LoTempio	ECE	NEU	jvelez@ll.mit.edu	MS	2007
Roman Trogan	ECE	NEU	trogan.r@neu.edu	MS	2007
David Insana	ECE	NEU	insanad@raytheon.com	PhD	2008
<b>Undergraduate Student Name</b>	<b>Major</b>	<b>Institution</b>	<b>Email</b>	<b>Degree (i.e. B.S, B.S.E.)</b>	<b>Anticipated Graduation Date</b>
Amanda Angell	ECE	NEU	ajangell@hotmail.com	BS	2007
Sarah Brown	ECE	NEU	ahsray@gmail.com	BS	2011
Eddie Vaisman	ECE	NEU	vaisman.e@neu.edu	BS	2012

## **I. Brief Overview of the Project and Its Significance**

Much of wave-based sensing and imaging of realistic problems has modeling at its core. For complex biological, anatomical, environmental, civil infrastructure, and even microelectronic systems, it is essential to understand the way that the fields configure themselves in the presence of nonuniformities. Before a particular sensor can be selected to probe, before an inversion method can be brought to bear, before an experimental protocol can be specified, it is essential to have an idea of what target and clutter signals are likely to exist, which wave features must be exploited, and what determines the dependences of observed fields on a particular excitation. For simple or idealized sensing, such as imaging discrete objects in a lossless, infinite, uniform background medium, the scattering is straightforward. But for the challenging and unsolved problems of concern to Gordon-CenSSIS, determining the particular non-intuitive field configuration may be the most difficult and important aspect to understanding the subsurface structure. The scattering information may be strong, but unless accurate models are used to determine propagation and scattering through random rough interfaces and layers, volumetric inhomogeneities, multiple targets, and strongly frequency dependent media, it is of little quantitative value.

We continue with the four broad challenges pursued since project inception: (1) fast computation of the mutual coupling effects of weak scatterers near rough interfaces; (2) accurate 3-D modeling of fully inhomogeneous media; (3) development of time domain dispersive biological tissue and soil models for microwave and mm-wave propagation and their use in mine and contaminant detection and breast cancer imaging, and; (4) simple modeling of very large ensembles of very weak scatterers, such as mitochondria within a cell, trees in a forest, or fish in the ocean. The first challenge has been addressed with the invention of the Semi-Analytic Mode-Matching (SAMM) method. The second challenge involves the theoretical foundation, sparse MATLAB implementation, parallel implementation, and extensive validation of the Finite Difference Frequency Domain (FDFD) model. The third has been addressed by the extensive searching, compilation, and fitting of multiple tissue type dielectric data. Finally, the fourth involves numerical experimental trials comparing gradually more complex models of distributed index-of-refraction variation to FDTD simulations.

Our collection of three-dimensional novel computational resources (dispersive FDTD, FDFD, and SAMM) provide for time-domain and frequency-domain modeling of electromagnetic (quasi-static through microwave, terahertz, and optical frequencies) in complex realistic, frequency-dependent, inhomogeneous media, including subcellular media (S1), human tissue (S3), and soil. While many computational models already exist throughout the scientific community (conventional FDTD, FEM, MOM, MRTD), their application to difficult realistic sensing and imaging problems with rough layers and distributed inhomogeneities is usually limited in ways which ignore key problem features. The fourth task, part of the computational modeling infrastructure, makes use of the spatial modal decomposition of the weak ensemble scattering, rather than discretization of the computational space. This novel approach then makes use of a Born-type approximation of the modal expansion of the ensemble to form a fast forward model for image inversion.

## **II. State of the Art, Major Contributions and Technical Approach**

### ***Semi Analytic Mode Matching (SAMM)***

The SAMM modeling algorithm quickly simulates rough-interface, half-space buried-object scattering from either plane wave on or borehole sources. SAMM uses moderately low-order modal superpositions of cylindrical or spherical waves, each of which satisfies the Helmholtz equation in its appropriate region (air, ground, or mine) and then matches all nonzero electric and magnetic field components at each interface by inverting a highly over-constrained dense linear matrix equation by singular value decomposition. That is, the set of spherical mode coefficients is found which best fits the boundary conditions in a least-squares sense. Extending features of the Method of Auxiliary Sources (MAS) [1, 2] the Generalized Multipole Techniques (GMT) [3,4], and the T-matrix method [5], this fast method provides self-consistent field solutions in the vicinity of the scatterers and interfaces. Fewer modes are needed than for MAS, GMT, or T-matrix because of its concentration on the local behavior of the fields in the region of interest.

The scalar Debye potentials  $\Pi^{e,m}(\mathbf{r})$  expressed in spherical coordinates are solutions to the Helmholtz equation  $(\nabla^2 + k^2)\Pi^{e,m} = 0$  [7] where  $\nabla^2$  is the Laplacian,  $k$  is the wave number and the electric and magnetic fields are related to  $\Pi^{e,m}(\mathbf{r})$  by the pair of equations:

$$\begin{aligned}\mathbf{E} &= \nabla \times (\mathbf{r}\Pi^m) - \frac{1}{i\omega\epsilon} \nabla \times \nabla \times (\mathbf{r}\Pi^e) \\ \mathbf{H} &= \nabla \times (\mathbf{r}\Pi^e) + \frac{1}{i\omega\mu} \nabla \times \nabla \times (\mathbf{r}\Pi^m)\end{aligned}\quad (1)$$

Three-dimensional solutions to the Debye potential are given by spherical mode superpositions:

$$\Pi^{e,m}(\mathbf{r}) = \sum_{p=1}^{N_{CSC}} \sum_{n=0}^N \sum_{m=-\min(n,M)}^{\min(n,M)} c_{nm,p}^{E,M} f_n(kr_p) P_n^m(\cos\theta_p) e^{im\phi_p} \quad (2)$$

Here,  $f_n(kr_p)$  is a spherical Bessel or spherical Hankel function of the first kind and  $P_n^m(\cos\theta_p)$  is an associated Legendre polynomial of order  $n$  and degree  $m$ . The coordinates  $\mathbf{r}$  and  $\mathbf{r}_p = (r_p, \theta_p, \phi_p)$  are related by  $\mathbf{r}_p = \mathbf{r} - \mathbf{c}_p$  where  $\mathbf{c}_p$  is the location of the  $p^{\text{th}}$  coordinate scattering center. The coefficients  $c_{nm,p}^{E,M}$  are determined by the SVD matrix inversion [8] for each mode  $(n, m)$  at each of the  $N_{CSC}$  coordinate scattering centers (CSCs) in each region, where a “region” is defined by a single complex dielectric or perfect conductor. As well as having a spatial location, each CSC may also have one or more user-specified orientations.

After extensive use of Bessel and Legendre recurrence relations [9], the Cartesian components of the electric and magnetic fields can be directly related to the Debye mode coefficients:

$$\begin{aligned}E_{\begin{Bmatrix} x \\ y \end{Bmatrix}} &= -\frac{1}{2} \begin{Bmatrix} i \\ 1 \end{Bmatrix} \sum_{n=0}^N \sum_{m=-\min(n,M)}^{\min(n,M)} F_n^m(\mathbf{r}, k) \left( \begin{Bmatrix} (n-1) \\ (2n-1) \end{Bmatrix} \eta c_{n-1,m-1}^E + \begin{Bmatrix} - \\ + \end{Bmatrix} \frac{(n-1)(n-m-1)(n-m)}{(2n-1)} \eta c_{n-1,m+1}^E - \frac{(n+2)}{(2n+3)} \eta c_{n+1,m-1}^E + \right. \\ &\quad \left. \frac{(n+2)(n+m+1)(n+m+2)}{(2n+3)} \eta c_{n+1,m+1}^E + c_{n,m-1}^M + \begin{Bmatrix} + \\ - \end{Bmatrix} (n-m)(n+m+1) c_{n,m+1}^M \right) \\ E_z &= \sum_{n=0}^N \sum_{m=-\min(n,M)}^{\min(n,M)} i F_n^m(\mathbf{r}, k) \left( \frac{(n+2)(n+m+1)}{(2n+3)} \eta c_{n+1,m}^E + \frac{(n-1)(n-m)}{(2n-1)} \eta c_{n-1,m}^E - m c_{nm}^M \right)\end{aligned}\quad (3)$$

The magnetic field equations are constructed by applying duality:  $\mathbf{E} \rightarrow \mathbf{H}$ ,  $\mathbf{H} \rightarrow -\mathbf{E}$ ,  $\Pi^m \rightarrow \Pi^e$ ,  $\Pi^e \rightarrow -\Pi^m$ ,  $c_{nm}^M \rightarrow c_{nm}^E$ ,  $c_{nm}^E \rightarrow -c_{nm}^M$ ,  $\epsilon \leftrightarrow \mu$ , and  $\eta \rightarrow 1/\eta$ . These six field components are used to match all boundary conditions at all interfaces. The series expansions in (2) and (3) are truncated by choosing  $N$  and  $M$ , the maximum radial and angular mode indices, such that  $n \leq N$  and  $|m| \leq M \leq n$ .

A particular geometry of interest is borehole dipole antenna scattering where the antenna and target are both located below ground. Subsurface sensing problems of this type include localizing underground waste, typified by dense, non-aqueous phase liquid (DNAPL) pools, detecting buried objects like unexploded ordnance (UXO), and identifying hidden structures, such as illicit tunnels.

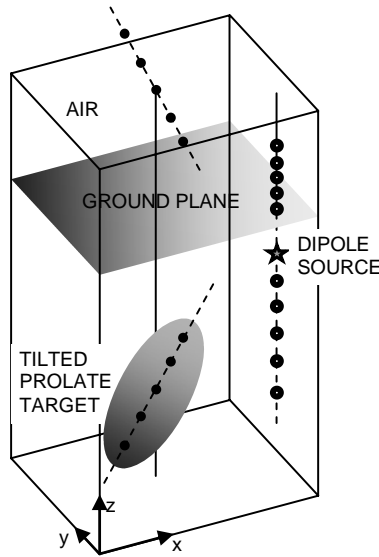


**Figure 1. Geometry of the tilted spheroidal target and dipole source, with CSC locations for the background dipole shown at the right (open circles) and CSC locations for the target shown on the left (closed circles).**

We start by ignoring the scatterer and simulate scattering from the borehole antenna under the ground plane. Two CSCs are the minimum needed for this background case. The waves refracted into the air region from the ground will have a longer wavelength than waves within the ground, so they appear to originate from a CSC that is not at the true dipole source location  $z = -d$  but is instead at the “effective dipole” location  $z = -nd$ . Here,  $n$  is the real part of the index of refraction ratio of the ground to air and waves generated at the effective dipole will therefore be valid *only in the air region*. The half-space boundary will also give rise to backscattering in the ground medium, which is sourced by the image of the dipole at  $z = +d$ , where this CSC is *valid in the ground region*. Additional CSCs may be placed along the  $z$ -axis in the vicinity of the two initial CSCs to improve the SAMM solution at the cost of greater computational time; 6 to 10 CSCs improve the error a few percent. These CSCs are shown on the right side of Figure 1 above and below the air-ground plane and aligned with the dipole source.

The target is now added to the simulation by reintroducing the correct dielectric constant within the target region. Discontinuities in fields across the target-ground interface act as sources for additional homogeneous, scattered half-space field solutions, which must exist in all regions of interest. For a small spherical scatterer, these additional field solutions are sourced by CSCs placed at the sphere’s center and at its image with respect to the ground plane. For larger, non-spherically shaped scatterers, other CSCs can be added within the scatterer and in the vicinity of its image in air to improve accuracy of the boundary matching; the 10 CSCs depicted on the left side of Figure 1 are examples of how these might be chosen.

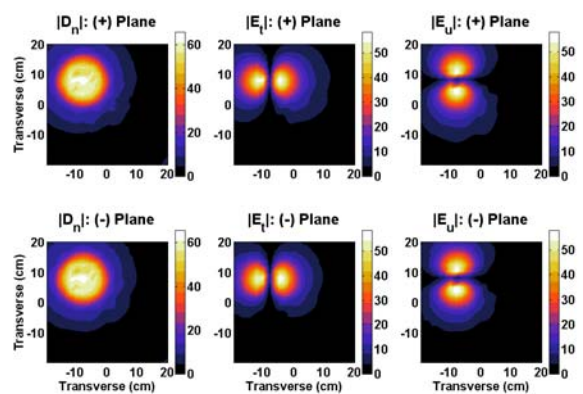
Note that decoupling the scattering from the background calculation allows fewer modes to be used at any given time but does not ignore multiple interactions, since these are modeled by continuing to refine the SAMM scattering solutions. Therefore this two-step process does *not* generate an approximate or perturbative solution but gives a self-consistent solution to the entire scattering problem.

Once the CSCs are chosen and, equally importantly, we designate in which regions these CSCs will be allowed to source waves, we place points on the surfaces of all interfaces in the region of interest. We must apply the appropriate continuity equations of all six Cartesian field components – since this “point matching” will be carried out numerically and not analytically. The appropriate spherical Bessel function  $f_n(kr) = j_n(kr)$  or (outward) spherical Hankel function  $f_n(kr) = h_n^{(1)}(kr)$  is specified for each mode “family” to ensure both that fields remain finite and radiation conditions hold in the far field. A dense matrix  $\mathbf{F}$  thus links the undetermined mode coefficients  $\mathbf{c}$  of (2) with boundary field mismatches  $\mathbf{b}$  arising in  $\mathbf{E}$  and  $\mathbf{H}$  at each point on the material interfaces through these continuity equations.

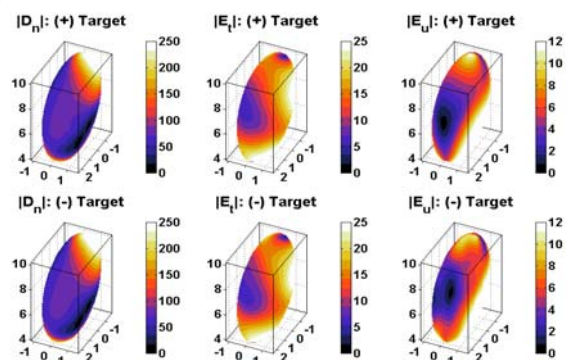
The over-constrained matrix equation  $\mathbf{F} \cdot \mathbf{c} = \mathbf{b}$  can now be inverted using singular value decomposition, selecting the (small) group of mode coefficients which best fit the (large) number of boundary conditions; the size of built-in error function  $\|\mathbf{F} \cdot \mathbf{c} - \mathbf{b}\|$  is an indication of how successfully SAMM has modeled scattering. The SAMM solution will be optimal in the nearfield region where it is properly constrained and inaccurate in the extrapolated region away from the fitting points. By sacrificing the need to have solutions valid in **all** regions of space, SAMM successfully describes scattering in a typical region of interest near the target.

As the total number of modes increases,  $\mathbf{F}$  becomes progressively more difficult to invert as there are so many local minima in the least squares error function that determining the true global minimum becomes subject to numerical error. One way to finesse this difficulty is to invert the matrix for a lower-order subset of  $\mathbf{F}$  containing fewer modes, find the optimal coefficient vector which satisfies the smaller least squares problem, and then add these low order  $\mathbf{c}$  components to total  $\mathbf{c}$ -vector. The procedure might be schematically given as follows: Define  $\mathbf{b}_{-1} = \mathbf{b}$  and  $\mathbf{F}_{-1} \cdot \mathbf{c}_{-1} = 0$ . Then, for increasing  $k$  such that  $0 \leq k \leq n$ : (1) Extract  $\mathbf{F}_k$  from the columns of  $\mathbf{F}_n$  and let  $\mathbf{b}_k = \mathbf{b}_{k-1} - \mathbf{F}_{k-1} \cdot \mathbf{c}_{k-1}$ , (2) Find  $\mathbf{c}_k$  such that  $\|\mathbf{F}_{k-1} \cdot \mathbf{c}_{k-1} - \mathbf{b}_k\|$  is minimized and (3) Let  $\mathbf{c}_k = \mathbf{c}_k + \mathbf{c}_{k-1}$ . With infinite machine accuracy, this iterative procedure would be equivalent to minimizing  $\|\mathbf{F} \cdot \mathbf{c} - \mathbf{b}\|$  in one step, but because  $\mathbf{F}$  is quite ill-conditioned for large total mode values, this procedure makes it possible to “steer” the unknown coefficient vector towards a physically appropriate solution, and ensures greater robustness of the SAMM algorithm.

The example of borehole scattering described in this section was chosen to have realistic dielectric properties with no special symmetry. Here, we simulate the probing of a contaminant pool with a dipole antenna buried below the surface of saturated sand. A 3D 30° prolate spheroidally shaped pool of a dense non-aqueous phase liquid (DNAPL) contaminant target having complex dielectric  $\epsilon = (2.63 + 0.016 i) \epsilon_0$  is buried in saturated wet sand with  $\epsilon = (20.7 + 1.4 i) \epsilon_0$ . The long axis of the pool is tilted 30 degrees about the  $y$ -axis towards the  $x$ -axis as shown in Fig. 1. A 1.4 GHz  $z$ -directed dipole antenna is placed to one side in a borehole at  $(-17h, 17h, -10h)$ , and we ignore the excavated borehole cavity itself as a source of scattering. Because the spatial grid size for the Half Space Born Approximation (HSBA) simulations used for comparative purposes is chosen to be  $h = \lambda/10 = 0.0047$  m in wet sand, it is convenient to describe all spatial dimensions for both SAMM and HSBA simulations in terms of  $h$ , though SAMM does



(a) Normal and tangential boundary fields on plane



(b) Normal and tangential boundary fields on target

**Figure 2. Excellent continuity of the normal  $D$  and tangential  $E$  fields is observed in the SAMM algorithm at both the planar and target interfaces for the buried DNAPL.**

not require a grid size. The center of the target pool is at  $(0, 0, -15h)$  and it has dimensions  $R_x = R_y = 2h$  and  $R_z = 5h$ , where the DNAPL-sand interface lies along  $(x'/R_x)^2 + (y'/R_y)^2 + (z'/R_z)^2 = 1$  in the tilted coordinate system. Numerical results are computed on planar  $y$ - $z$  “slices” at  $x = 8h$  and  $x = 24h$ . The SAMM algorithm uses 841 matching points, spaced approximately  $3h$  apart, placed over an  $85h$  by  $85h$  rectangular section of the air-ground planar (spaced approximately  $\frac{1}{2}h$  to  $2h$  apart along the spheroidal surface). HSBA simulations use a 3D volume discretized by  $41 \times 41 \times 51$  points with uniform grid spacing  $h$ . The normal component of  $\mathbf{D} = \epsilon\mathbf{E}$  and both tangential components of  $\mathbf{E}$  ( $E_t$  and  $E_u$ ) are plotted in Figure 2a for the air-ground planar interface at  $z = 0$ , where the upper row of plots is specified at  $z = 0^+$  and the lower row of plots at  $z = 0^-$  and three field components are demonstrably continuous.

Similarly, Figure 2b depicts continuity of  $D_n$ ,  $E_t$ , and  $E_u$  on the ground-DNAPL prolate spheroidal target interface. Comparison of SAMM to the Green’s function-based HSBA in Figure 3 demonstrates excellent agreement between the two methods. A Matlab implementation of SAMM running on a laptop takes about one-tenth the computational time of a similar implementation of HSBA.

The SAMM algorithm is a useful nearfield half-space algorithm, orders of magnitude faster than finite difference methods and requires substantially less computational overhead. SAMM has wide applicability and may be used for irregularly shaped boundaries and for both metallic and dielectric objects, multiple scatterers and rough surfaces. By choosing CSC locations/orientations properly and treating background half-space scattering separately, a full 3D SAMM simulation may be quickly obtained of underground (borehole) dipole sources of order  $N^2$  computational size. SAMM and HSBA, two very different computational methods, agree well in a non-ideal asymmetric test case.

While SAMM is not applicable at large distances from a given scatterer region of interest, it accurately models scattering within and immediately around the scatterer, as well as on the interface and in the surrounding media on both sides of it. SAMM can be applied iteratively, generating approximate fields solutions quickly that can be progressively refined for higher accuracy.

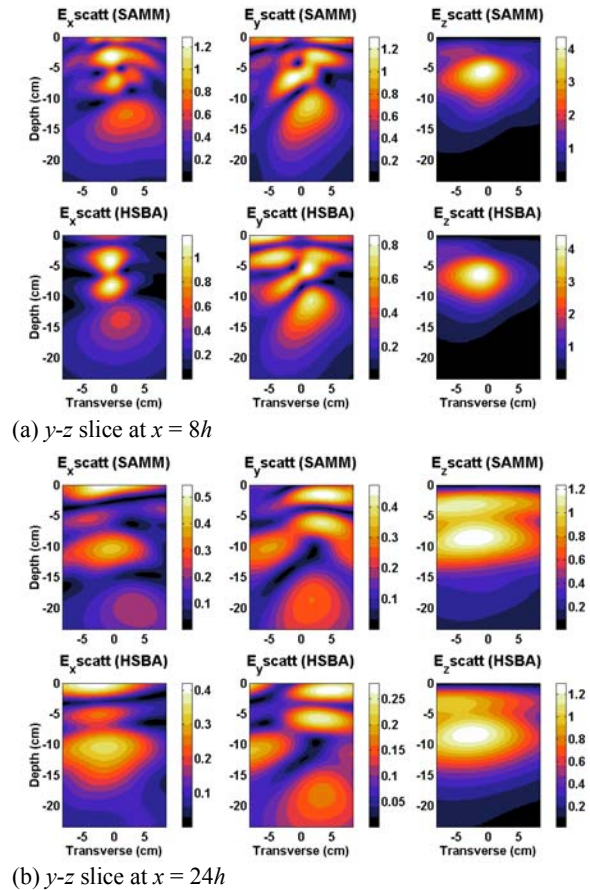


**Figure 3. SAMM (first and third row) versus HSBA (second and fourth row) simulations for buried DNAPL target. Slices are obtained at  $x = 8h$  and  $x = 24h$ . The three electric field components are plotted for both methods.**

### ***Finite Difference Frequency Domain Forward and Inverse Modeling (FDFD)***

We have developed a new algorithm for the electromagnetic inverse scattering problem in inhomogeneous media using Matlab sparse matrix routines implementing the finite difference frequency domain (FDFD) model [10], referred to as the FDFD-based inversion method. The key issue of this method is to build a linear expression for the inverse problem from the FDFD forward model by using the vector-based Born approximation of single scattering of incident field. The advantage of the FDFD-based approach is that no Green's function is required, so it can be readily applied to strongly layered or discontinuous backgrounds. This inversion algorithm is tested for microwave subsurface object detection by comparing with the conventional inversion procedure using an integral equation Green function-based Born Approximation (GFBA). This electromagnetic scattering inverse algorithm is easily implemented and robust to the heterogeneity of the background.

Numerical experiments have been conducted for two types of 2D applications: 1) Multiple borehole antenna source and receiver configurations for the detection of buried objects in soil; and 2) Microwave breast tumor detection. Fig. 4 shows the geometry for a borehole case, with contrasting permittivity of dielectric contaminant pools near the ground interface. The reconstructions, shown in Fig. 5, compare single sided and two-way inversions using the FDFD-Based method and the conventional integral equation Green's function method. The results are comparable, but the novel method does not require the knowledge of a Green's function and uses fewer computational resources.

### ***Modeling Dispersive Media in the Time Domain***

Propagation in dispersive media has been a research subject of interest for many years. Time reversal in these kinds of media is an interesting subject in a variety of inverse problems such as biomedical or environmental applications. The first thing in addressing these problems is defining an accurate model for dispersive material which is valid for a wide range of frequency.

In our work, a new accurate parametric rational Z-transform conductivity model, called Four-zero, is developed and implemented in FDTD to solve both forward and reverse propagation problems in dispersive media. One of the challenging issues in developing a

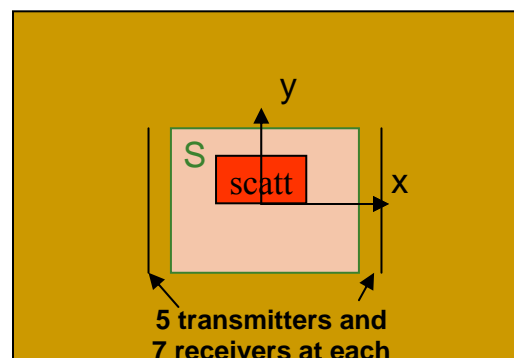


**Figure 4. Geometry of 2D half-space scattering problem, with rectangular contaminant pool ( $\epsilon' = 2.9$ ) in moist uniform soil ( $\epsilon' = 2.25$ )**

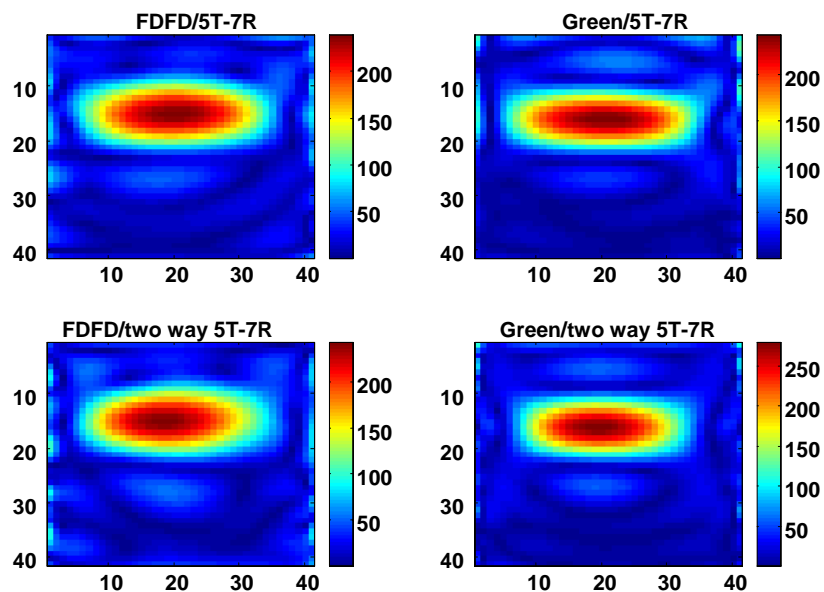


**Figure 5. 2-D half-space reconstruction of rectangular contaminant pool of Figure 4 for FDFD-Based method (left) and conventional Green's function (right) Born Approximations.**

new propagation model is its stability. In FDTD algorithm, all media, lossless or lossy, are subjected to the Courant stability condition which determines the lower bound on spatial grid spacing in terms of time steps. In dispersive media, we are faced with a more restricted stability condition of Von-Neumann type, which should be solved analytically in the z-plane and plays a significant role in choosing the model parameters with optimized stability. We address this issue by a comprehensive stability analysis.

We develop a time-reversal method to predict the propagation in dispersive media modeled by our Four-zero conductivity model. The inherent instability in the reversal algorithm necessitates a stabilization technique. A novel comprehensive gain-removal method is developed for implementation in various media, lossless or lossy, non-dispersive or dispersive, for forward propagation as well as time reversal. This technique removes the requirement to satisfy the stability condition.

The gain-removal method is based on the fact that in any medium (lossless or lossy) with spatial and temporal gridding parameters exceeding stability condition, we can enforce gain-removal (amplitude attenuation) to the traveling wave to stabilize the propagation. This results in a new set of stable wave equations for electric and magnetic fields which can be solved computationally. At the last step, removed gain can be inserted directly by multiplying the amplitude by the gain.

The numerical results indicate the successful application of the new Z-transform modeling of dispersive materials by the Four-zero rational formulation used in implementation of the forward and reverse FDTD algorithm with the gain-removal stabilization technique (see Figure 6).

### ***Weak Scatterer Ensemble Modeling***

Non-invasive assessment of the health of an embryo or a single cell is an open issue of critical importance for the success of certain procedures like in vitro fertilization (IVF). A three-dimensional understanding of the investigated structure, such as how various organelles are distributed within the cell, is necessary to achieve this goal. Advanced microscopy techniques can provide both amplitude and phase information from multiple views, but obtaining detailed volumetric information is still challenging. In particular, imaging mitochondria is usually quite

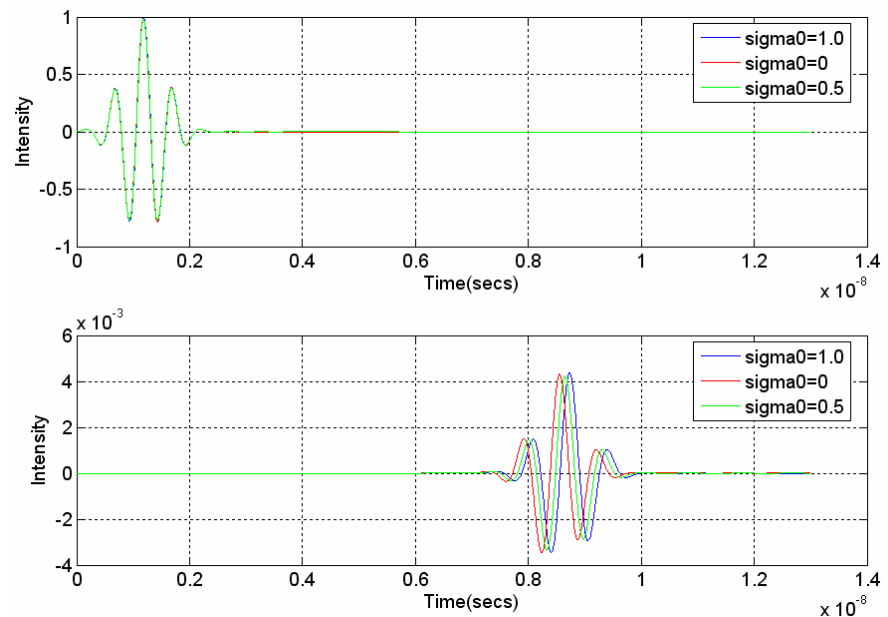


**Figure 6. A comparison of one-dimensional time-domain wave propagation in lossy, dispersive breast fat tissue using the conventional method and the artificially induced loss method. Top plot indicates the initial 2 GHz modulated Gaussian excitation signal at the left edge of the medium. Bottom plot shows the attenuated and slightly distorted response 500 space steps (each step being 2mm) into the tissue medium. The artificial loss (either  $\sigma = 0.5$  or  $1.0$ ) is compensated for after the wave propagates, and returns the signal to its correct amplitude and shape. There is a small advance in time, which must also be corrected.**

difficult since there may be tens of thousands of these tiny, low-contrast scatterers overlapping each other within the cell.

When the inhomogeneities in an investigated object are comparable in size to the wavelength of the probing signal, as is the case of a cell being illuminated by a laser operating in or near the visible spectrum, techniques based on straight ray assumptions suffer from the effects of diffraction and refraction. In this case, diffraction tomography techniques considering wave propagation and diffraction phenomena must be employed.

Although the electromagnetic properties of cellular structures exhibit slight variations relative to the background, classical optical diffraction tomography techniques based on the Born or Rytov approximations are not suitable to image these objects since their electrical sizes are quite large when probed in or near the visible spectrum, and the observed scattered light is in the far zone.

In this study, we present a novel method to image these objects in two dimensions. It is based on the expansion of the target object function in terms of Fourier-Bessel basis functions with corresponding, unknown expansion coefficients, and an alternative approximation for the total fields within the scatterer. Unlike the Born and Rytov approximations, this new approximation satisfies the continuity of the total tangential fields along the object support-background boundary for each circular mode using the known incident and observed scattered fields, and takes into account the fact that the refractive index distribution along structures being investigated varies slightly around a known mean value. The resulting ill-posed linear system of equations is solved via truncated singular value decomposition (TSVD) for the unknown expansion coefficients. This approach can be readily extended to more realistic 3D cases.

We validate the proposed method by comparing its performance with that of the existing diffraction tomography (DT) techniques. A number of simulations, involving plane wave scattering through various 2D objects, such as radial cylinders, random phantoms, and finally cell models with miscellaneous mitochondrial distributions, are performed. Except for the radial cylinders for which an iterative, analytical forward solution is available, the Finite-Difference Time-Domain (FDTD) method is used in the simulations. Basic principles of the FDTD method, such as total-field scattered-field formulation, near-to-far-field transform, and PML absorbing boundary conditions are employed in these simulations. The far zone scattered fields obtained with these simulations are then utilized to reconstruct the probed objects via both the proposed method and the conventional DT techniques. Qualitative and quantitative superiority of the proposed technique is demonstrated, as shown in Figure 7.

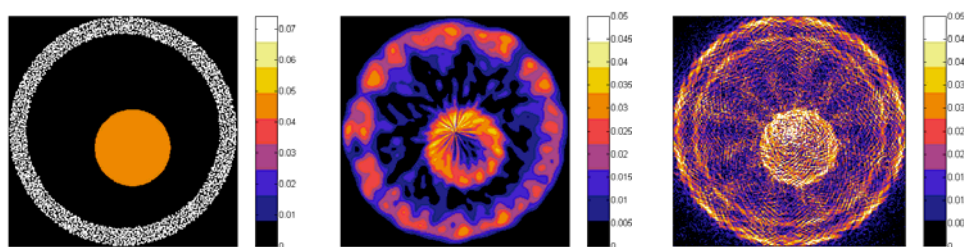


**Figure 7. Two-dimensional cell with cortical mitochondria distribution. Left to right: test geometry, reconstruction based on twelve farfield views, diffraction tomography reconstruction.**

### **III. Gordon-CenSSIS Strategic Goals and Legacy**

The development of general-purpose computational models to address the system area applications supports the Center's strategic goals and will leave a legacy of powerful tools that

while designed for a handful of specific problems, can directly be extended to future realistic sensing problems.

#### **IV. Future Plans**

##### **A. Gordon-CenSSIS Computational Infrastructure**

- Combine various modeling codes, with the help of R3 researchers, into a computational modeling toolbox.
- Continue to coordinate with project SoilBED-B to establish a Virtual SoilBED environment.

##### **B. Semi-Analytic Mode Matching**

- Automate 3-D irregular interface modeling in SAMM code.
- Use SAMM to quickly determine half space and layered Green's functions for canonical target objects.

##### **C. FDFD**

- Develop and quantify the effectiveness of FDFD-based Born Approximation.

##### **D. Dispersive Electromagnetic Biological Tissue Modeling**

- Validate dispersion model theory for multiple tissues for stable time-reversal analysis.
- Continue collaboration with the Dartmouth College Breast Imaging Center's microwave spectroscopic imaging program to develop optimal sensor configuration and forward models for reconstruction algorithms.

##### **E. Sub-Cellular Optical Scattering Modeling**

- Adapt this forward model for use in reconstruction algorithms.
- Establish detectability criteria for clumped versus dispersed microscatterers.
- Apply the ensemble weak scatterer paradigm to non-uniform media, such as objects in forests.

#### **V. Broader Impact**

The models are being developed to consider the non-ideal nature of specific problems, which are common to problems in other areas. For example: dispersive soil electromagnetic wave propagation models are easily extended to biological tissue models, and perhaps even to models of acoustic waves in seawater; large ensemble weak scattering such as mitochondria in a cell may extend to trees in a forest.

#### **VI. Technology Transfer**

As this is a fundamental science project, with various modeling algorithms and codes used to support the broad mission of Gordon-CenSSIS, it does lend itself to commercial products. There has been some interest among the academic community to implement specific dispersive models for tissue types (such as breast tissue). MIT Lincoln Lab, TransTech Systems and Raytheon have each expressed interest in our research, both in partnering on grants and contracts as well as technical interchange. The effort necessary to commercialize any of the codes for general-purpose use is beyond the scope of this effort.

**VIII. References Cited**

- [1] Morgenthaler, A. and Rappaport, C., “Scattering from dielectric objects buried beneath randomly rough ground: Validating the semi-analytic mode matching algorithm with 2-D FDFD,” *IEEE T. Geo. Rem. Sens.*, vol. 39, no. 11, pp. 2421-2428, Nov. 2001.
- [2] Morgenthaler, A. and Rappaport, C., “Detecting nonmetallic mines under rough ground using semi-analytic mode matching,” *Int’l J. of Subs. Sens. Tech. Appl.*, vol. 2, no. 3, pp. 231-247, Jul. 2001.
- [3] Morgenthaler, A. and Rappaport, C., “The semi-analytic mode matching (SAMM) algorithm for efficient computation of scattered near fields from 3D dielectric targets buried in lossy soil,” *IEEE Int’l Ant. Prop. Symp.*, vol. 3B, pp. 92-95, Wash., DC, July 2005.
- [4] Firoozabadi, R., Miller, E. L., Rappaport, C. M. and Morgenthaler, A. W., “A new inverse method for simultaneous reconstruction of object buried beneath rough ground and the ground surface structure using SAMM forward model,” *Proceedings of SPIE 5674: Computational Imaging III*, San Jose CA, pp. 382-393, March 2005.

- [5] Silver, S. Microwave Antenna Theory and Design. Rad. Lab Series No. 12. New York: McGraw Hill, 1949.
- [6] Kong, J. A. Electromagnetic Wave Theory. New York: John Wiley & Sons, 2002.
- [7] Stratton, J. A. Electromagnetic Theory. New York: McGraw-Hill Book Co., Inc., 1941. Pp. 392-419.
- [8] Press, W. H., Vetterling, W. T., Teukolsky, S. A. and Flanner, B. P., Numerical Recipes in C. 2<sup>nd</sup> Ed. London: Cambridge Univ. Press, 1992. Pp. 59-70, 240-54, 496-509, 549-57.
- [9] M. Abramowitz and I. A. Stegun. Handbook of Mathematical Functions. New York: Dover, 1972.
- [10] Dong, Q., Zhan, H., and Rappaport, C., “Efficient 3D Finite Difference Frequency-Domain Modeling of Scattering in Lossy Half-space Geometries”, *IEEE Antenna and Propagation Symposium*, Honolulu HI, pp. 1789-1792, June 2007.

## **VII. Documentation**

### **A. Publications Acknowledging NSF Support**

#### ***Refereed journal publications***

1. Firoozabadi, R., Miller, E., Rappaport, C., and Morgenthaler, A., “Subsurface Sensing of Objects Under a Randomly Rough Surface Using Scattered Electromagnetic Field Data,” *IEEE Transactions on Geoscience and Remote Sensing*, vol. 45, no. 1, pp. 104-117, Jan. 2007.
2. Ratilal, P., Andrews, M., Donabed, N., Galinde, A., Rappaport, C., and Fenneman, D., “Model for continuously scanning ultrasound vibrometer sensing displacements of randomly rough vibrating surfaces,” *The Journal of the Acoustical Society of America*, vol. 121, no. 2, pp. 863-878, Feb. 2007.
3. Zhan, H., Rappaport, C., Farid, M., Alshawabkeh, A. and Raemer, H. “Scale Model Experimental Validation and Calibration of the Half-Space Green’s Function Born Approximation Model Applied to Cross-Well Radar Sensing,” *IEEE Transactions on Geoscience and Remote Sensing*, vol. 45, no. 8, pp. 2423-2429, Aug. 2007.
4. Rappaport, C., “Accurate Determination of Underground GPR Wavefront and B-Scan Shape from Above Ground Point Sources,” *IEEE Transactions on Geoscience and Remote Sensing*, vol. 45, no. 8, pp. 2429-2434, Aug. 2007.
5. Rappaport, C., “A Dispersive Microwave Model for Human Breast Tissue Suitable for FDTD Computation,” *IEEE Antennas and Wireless Propagation Letters*, vol. 6, pp.179-181, 2007.
6. Angell, A. and Rappaport, C., “Computational Modeling Analysis of Radar Scattering by Clothing Covered Arrays of Metallic Body-Worn Explosive Devices,” *Progress in Electromagnetics Research*, vol. 76, pp. 285-298, 2007.

**Refereed conference proceedings**

1. Karbeyaz, E., and Rappaport, C., “Modeling and Inversion of Weakly Scattering Structure in Electrically Large Cells,” *Proceedings of the Applied Computational Electromagnetics Society*, Verona, Italy, pp. 895-903, Mar. 2007.
2. Angell, A., and Rappaport, C., “Computational Modeling Analysis of Radar Scattering by Metallic Body-Worn Explosive Devices Covered with Wrinkled Clothing,” *IEEE Int’l Microwave Symp.*, Honolulu HI, pp. 1943-1946, Jun. 2007.
3. Lorenzo-Martinez, J.A., Rappaport, C., Sullivan, R., and Garcia-Pino, A., “A Bistatic Gregorian Confocal Dual Reflector Antenna for a Radar Bomb Detection System,” *IEEE AP-S International Symposium*, Honolulu, HI, Jun. 2007.
4. Lorenzo-Martinez, J.A., Rappaport, C., and Garcia-Pino, A., “Reflector Antenna Discrete Distortion Determination: An Iterative Field-Matrix Solution,” *IEEE AP-S International Symposium*, Honolulu, HI, Jun. 2007.
5. Lorenzo-Martinez, J.A., Rappaport, C., and Garcia-Pino, A., “Reflector Antenna Diagnosis Using Near-Field Data,” *IEEE AP-S International Symposium*, Honolulu, HI, Jun. 2007.
6. Gonzalez-Valdes, B., Lorenzo-Martinez, J.A., Garcia-Pino, A., and Rappaport, C., “Zooming Techniques for a Gregorian Confocal Dual Reflector Antenna,” *IEEE AP-S International Symposium*, Honolulu, HI, Jun. 2007.
7. Gonzalez-Valdes, B., Martínez-Lorenzo, J. A., Pino, A. G. and Rappaport, C. M., “Zooming and scanning a beam by hybrid mechanical-electronic pointing systems”, *ESA Antenna Workshop on Space Antenna Systems and Technologies*, Noordwijk, Netherlands, Apr. 2007.
8. Karbeyaz, E., and Rappaport, C., “Modeling and Inversion of Weakly Scattering Subcellular Inhomogeneities in Electrically Large Cells,” *IEEE AP-S International Symposium*, Honolulu, HI, Jun. 2007.
9. Dong, Q., Zhan, H., and Rappaport, C., “Efficient 3D Finite Difference Frequency Domain Modeling of Scattering in Lossy Half-Space Geometries,” *IEEE AP-S International Symposium*, Honolulu, HI, Jun. 2007.
10. Winton, S., and Rappaport, C., “Reduced Deposition and Improved System Performance of Radiating System in Presence of Human Head,” *IEEE AP-S International Symposium*, Honolulu, HI, Jun. 2007.
11. Martinez-Lorenzo J. A, Rappaport C. M. and Pino, A. G. “An Iterative-Field-Matrix Method for Reflector Antenna Distortion Determination”, *URSI International Symposium on Electromagnetic Theory*, Ottawa ON, Jul. 2007.
12. Zhan, H., Morgenthaler, A., Dong, Q., Rappaport, C. and Miller, E.L., “Half-Space Born Approximation Modeling and Inversion for Cross-Well Radar Sensing for Contaminants in Soil,” *IEEE Int’l Geoscience and Remote Sensing Symposium*, Barcelona, Jul. 2007.
13. Morgenthaler, A., Zhan, H., and Rappaport, C., “Semi-Analytic Mode Matching (SAMM) Algorithm for Efficient Computation of Nearfield Scattering in Lossy Ground from Borehole Sources,” *IEEE Int’l Geoscience and Remote Sensing Symposium*, Barcelona, Jul. 2007.

14. Rappaport C. M., Martinez-Lorenzo, J. A., Sullivan, R., and Angell, A., “Modeling millimeter-wave detection of body worn explosives”, Gordon Research Conference on detecting illicit substances: explosives and drug, Big Sky MT, Aug. 2007.

**B. List of Relevant RICC 2007 Posters**

1. Morgenthaler, Ann, Zhan, He, Rappaport, Carey, “The Semi-Analytic Mode Matching (SAMM) Algorithm for Efficient Computation of Nearfield Scattering in Lossy Ground from Borehole Sources,” *presented at the Gordon-CenSSIS Research Industrial Collaboration Conference*, Boston, MA, Oct. 2007.
2. Dong, Qiuzhao, Rappaport, Carey, "Matlab-based FDFD Modeling for Microwave Breast Imaging," *presented at the Gordon-CenSSIS Research Industrial Collaboration Conference*, Boston, MA, Oct. 2007.
3. Brown, Sarah, Rappaport, Carey, Martinez-Lorenzo, Jose Angel, "Optimization of Antenna Excitations in High Field MRI," *presented at the Gordon-CenSSIS Research Industrial Collaboration Conference*, Boston, MA, Oct. 2007.
4. Sullivan, Richard, Angell, Amanda, Rappaport, Carey, Jose Martinez-Lorenzo, "Modeling Millimeter-Wave Detection of Body-Worn Explosives," *presented at the Gordon-CenSSIS Research Industrial Collaboration Conference*, Boston, MA, Oct. 2007.
5. Simon, Blair, and DiMarzio, Charles "Simulation of Imaging with a Theta Line-Scanning Confocal Microscope," *presented at the Gordon-CenSSIS Research Industrial Collaboration Conference*, Boston, MA, Oct. 2007.
6. Belli, Kimberly, Zhan, He, Wadia-Fascetti, Sara, and Rappaport, Carey, “Comparison of the Accuracy of 2D versus 3D FDTD Air-Coupled GPR Modeling of Bridge Deck Deterioration”, *presented at the Gordon-CenSSIS Research Industrial Collaboration Conference*, Boston, MA, Oct. 2007.

**C. Seminars Workshops, Short Courses**

“2D Modeling of Wave Propagation and Scattering with the FDFD Method”	1/18/07	Univ. of Puerto Rico at Mayaguez	Presenter
“General Teaming Approaches and Considerations for the NIH Superfund Proposal”	3/27/07	Univ. of Puerto Rico Medical Campus	Presenter
“Electromagnetic Wave Propagation Through Inhomogeneous Media”	5/09/07	AFOSR Workshop, Hanscom AFB	Presenter
“FDTD and FDFD Modeling for Electromagnetic Wave Applications”	6/28/07	Schlumberger Doll Research Lab	Presenter
“Millimeter-Wave Radar Detection of Concealed Body-Worn Explosives”	12/18/07	Lincoln Lab workshop on fostering collaboration	Presenter